

# EXPRESS-EVALUATION OF THE QUALITY OF PRODUCING CATERPILLAR TRACKS BY THE RESULTS OF COERCIVE FORCE MEASUREMENT

O.P. Gopkalo<sup>1</sup>, O.Ye. Gopkalo<sup>1</sup>, M.P. Zemtsov<sup>1</sup>, Ye.V. Kovalenko<sup>2</sup>, V.E. Bodunov<sup>1</sup>

<sup>1</sup>G.S. Pisarenko Institute for Problems of Strength of the NAS of Ukraine

2 Timiryazievskaya Str., 01014, Kyiv, Ukraine

<sup>2</sup>“SPC Aviation Systems of Ukraine” LLC

8 Redutna Str., 01015, Kyiv, Ukraine

## ABSTRACT

Coercimetric testing revealed essential differences in metal structure in the subsurface layer of experimental caterpillar tracks. Obtained experimental results of 4-point bend testing of experimental caterpillar tracks from steels which somewhat differ by their chemical composition, confirmed the possibility of application of nondestructive coercimetric testing for assessment of the initial structural state and level of loading of the metal, which characterizes the degree of obtained damage after loading. Metal of a sound track from steel of 110G13L type in the initial condition should have negative values of the coercive force that is ensured by its optimal structural state. This circumstance can provide substantiation for introducing coercimetric testing for express-evaluation of the quality of castings and their heat treatment.

**KEYWORDS:** caterpillar tracks, structuroscope, coercive force, structural state

## INTRODUCTION

Mechanical properties of metal products depend on its composition and structural state. In this work there was used a nondestructive magnetic method for evaluation of quality of structural state of metal of experimental caterpillar tracks of Hadfield type austenite steel (with some deviation of composition) in initial condition as well as after standard 4-point bend testing by the results of coercive force measurement. Coercive force is an integral characteristic of a structural state of metal which depends on content and concentration of chemical elements in metal and phase and structural constituents.

Table 1 provides composition of Hadfield type steel (110G13L steel grade according to DSTU 8781:2018).

Steel 110G13L has typical for austenite steels toughness and ductility at sufficiently high strength. At low hardness 110G13L steel has extremely high wear resistance at friction with pressure and impacts. This is explained by strengthening (hardening) of austenite at plastic deformation in process of work, i.e. this steel has increased tendency to hardening (sufficiently higher than in common ones with the same hardness). Presence of significant ductility margin of

steel 110G13L allows redistributing the stresses of the most loaded areas of the track that provides high integrity of the product.

Hardening results in increase of wear resistance, therefore steel 110G13L is difficult to treat by cutting tools and parts from it are mostly produced by casting without mechanical treatment. Under conditions of purely abrasive wear (for example, at sand friction) there is no effective hardening of steel 110G13L that leads to increase of parts wear-out. Due to unique mechanical properties steel 110G13L has found wide application in manufacture of wear-resistant parts of machines.

## PURPOSE OF WORK

Lies in experimental check of the possibility of application of coercimetric testing for express-evaluation of the quality caterpillar tracks manufacture.

## INFLUENCE OF COMPOSITION AND STRUCTURAL STATE ON MECHANICAL PROPERTIES OF 110G13L STEEL

Regardless the fact that strength, ductility and wear resistance of high-manganese steels to a great extent

**Table 1.** Composition of steel 110G13L according to DSTU 8781:2018

Weight fraction, %								
C	Si	Mn	Cr	Ni	Cu	S	P	Fe
0.9–1.4	0.3–1.0	11.5–15.0	Up to 1.0	Up to 1.0	Up to 0.3	Up to 0.05	Up to 0.2	~83

**Table 2.** Dependence of mechanical properties of steel 110G13L of different manufacturers on composition (standard values are given in brackets)

Composition, %	Manufacturer						
	No. 1	No. 2	No. 3	No. 4	No. 5	No. 6	No. 7
C (0.9–1.4)	0.98	0.94	1.05	1.15	0.95	0.97	1.05
Mn (11.5–15)	11.60	10.50	12.69	13.13	13.47	12.35	13.40
Si (0.8–1)	0.66	0.64	0.46	0.51	0.44	0.51	0.44
Cr (up to 1.0)	0.10	0.59	0.15	0.39	0.14	0.13	0.11
Ni (up to 1.0)	0.18	0.27	0.20	0.16	0.21	0.16	0.27
P (up to 0.12)	0.025	0.057	0.029	0.048	0.025	0.028	0.027
S (up to 0.05)	0.012	0.004	0.005	0.004	0.007	0.006	0.005
Cu (up to 0.3)	0.18	0.17	–	–	0.17	0.12	0.19
Characteristics							
$\sigma_b$ , MPa	790	610	710	660	850	790	690
$\sigma_{0.2}$ , MPa	370	400	440	455	350	375	355
$\delta$ , %	38	21.5	24.5	21.5	43	37	27
$\psi$ , %	29	18.5	41	29	39	37	31
$KCU^{20}$ , J/cm <sup>2</sup>	242	265	325	234	261	258	262
$KCU^{-60}$ , J/cm <sup>2</sup>	90.5	39	159	45	–	–	–
Hardness, <i>HB</i>	202	202	187	187	–	–	–
Grain size number	3	1	1	0	–	–	–

are determined by DSTU and technical conditions of different suppliers, sufficiently wide variation of content in metals is allowed even of such main alloying elements as C, Mn, Si, S, P that is clearly not justified [1]. To increase wear resistance of castings of 110G13L steel its alloying with titanium (to 0.05 %), vanadium (to 0.3 %), molybdenum (to 0.2 %) [2] is allowed. Vanadium alloying increases up to 30 % wear resistance and decreases cold resistance, however affects strength characteristics.

It is determined that addition of 2 % of vanadium to 110G13L steel results in five times increase of wear resistance at conservation of impact toughness. Chromium alloying (to 1.5 %) [2] rises strength and wear resistance properties of steel. At that ductility and toughness are little bit reduced, however remain at the level that exceeds these characteristics for common high-manganese steel and provide normal operation of products with increase of wear resistance on average at 15–20 %. In other words, desired indices of wear resistance can be significantly increased [3] at up to 1.0 % chromium alloying of steel 110G13L (within the limits of DSTU requirements).

Increase of content of Cr, Si, Ni, Cu and decrease of Mn concentration in metal provoke rise of the coercive force values. Content in steel of carbon in 0.9–1.0 % limits and phosphorous not more than 0.5–0.55 % minimizes impact toughness. Increase in steel of silicon content decreases impact toughness. Maximum indices of impact toughness at 0.5 % silicon content [3].

The main problem for production of quality castings is selection of casting technology and heat treat-

ment. Quality heat treatment is a key factor for obtaining the desirable metal structures.

Heat treatment of steel 110G13L is regulated by DSTU 8781:2018 — austenization at 1050–1100 °C temperature with cooling in cold water (not more than 30 °C). It should be noted that columnar and dendritic cast structure can not be completely removed by heat treatment and has negative effect on impact toughness, resistance to abrasive wear and dynamic loadings. Increase of hardness promotes increase of coercive force values [2].

Table 2 gives the data [4] of dependence of mechanical properties of steel 110G13L of different manufacturers on composition.

Provided results show that difference of composition of the track metal of different manufacturers promotes scatter of mechanical characteristics on average in the following limits, namely  $\sigma_b$  — 32.9 %;  $\sigma_{0.2}$  — 26.1 %;  $\delta$  — 66.7 %;  $\psi$  — 65.6 %;  $KCU^{20}$  — 32.6 %;  $KCU^{-60}$  — 121.2 %; hardness, *HB* — 7.7 %. Concentration of Mn and Si is lower of the standard values in castings of manufacturer No. 2, promotes the most decrease of strength characteristics  $\sigma_b$ , relative constriction at tension  $\psi$  and impact toughness  $KCU$  at –60 °C in relation to similar indices of metal of castings of other manufacturers [4].

Dependence of Mn/C index for steel 110G13L shows that its growth rises impact toughness. It is believed that the optimum relationship of Mn/C is not less than 10.0. The maximum indices of impact toughness are reached at Mn/C relationship in 12–13 range. P + 0.4C index characterizes an effect of phosphorous which is desirable to be not more than 0.5 %.

Increase of this index for steel 110G13L promotes decrease of impact toughness. At P+0.4C more than 0.5 % the steel is susceptible to crack formation [1].

Nondestructive methods of testing are widely used for diagnostic of the quality of structural state of the products metal in initial condition and evaluation of metal damageability in process of structure operation. Work [5] provides the example of diagnostics of the level of damageability of metal of the caterpillar tracks at their standard 4-point bend testing. The tracks with optimum structural state of metal (austenitic structure) are characterized with absence of magnetic properties of metal in initial condition and, respectively, zero values of coercive force. Elastic-plastic loading deformation provokes increase of the coercive force values and distribution diagrams look like approaching the circle.

Since coercive force is an integral characteristic of metal structural state which depends on content and concentration of elements, phase and structural constituents then application of coercimetric testing allows express-evaluation of the tracks metal quality.

#### PROCEDURE OF EXPERIMENTAL INVESTIGATIONS

The experimental investigations lied in determination of distribution of the values of coercive force along a surface of 13 experimental caterpillar tracks of steel 110G134L (with some deviation of composition from regulated one) of two different manufacturers in initial state and after 4-point bend testing.

Figure 1 shows the general view of tracks before testing with digital identification of points for further measurement of the coercive force.

Measurement of the coercive force on the track surface in the typical points was carried out using strukturoscope KRM-Ts-K2M (developer “Special Scientific Engineering LLC”, Kharkiv). Since the tracks have complex volumetric configuration with internal cavity (at wall thickness 4–5 mm), then a compact probe D12 with measurement base 12×12 mm and magnetization depth to 1 mm was used for measurement of the coercive force with registration of possible hardening of the surface layers of metal under operation. Application of such probe allows measurement of the values of coercive force in very limited

local areas of the track, which has sufficiently complex surface geometry. Measurement of the values of coercive force with D12 probe showed presence of significant scatter of  $H_c$  in the different points of the experimental track surface. In this work in order to obtain more integral values of the coercive force in significantly larger volumes of metal (27×25×4 mm) D27 probe was used. It has measurement base of 27 mm and magnetization depth to 4 mm that allows significantly reducing scatter of the measured values.

Measurement of the coercive force lies in initial magnetization of the metal till saturation with the following next complete demagnetization and further magnetization with magnetic field of opposite polarity for neutralizing the residual magnetism and measurement of  $H_c$  values. Duration of a cycle for coercive force determination makes 10 s. It should be noted that in presence of anisotropy of the metal structure, including after plastic deformation, the values of coercive force in the investigated points are changed at variation of measurement directions (orientation of magnetic poles of the probe relatively to the examined surface). Due to this measurement of  $H_c$  values was carried out at each 45° turn relatively previous measurement (in total 8 measurements at orientations: 0, 45, 90, 135, 180, 225, 270, 315°), where a direction of measurement of the values of coercive force  $H_{c||}$  (0, 180, 360°) was taken across the track (along the track chain) and  $H_{c\perp}$  (90, 270°) — along the track (across the track chain). Measurement of the values of coercive force in typical points of the surface of the tracks was carried out in initial condition and after standard 4-point bend tests.

Testing of tracks in initial condition for 4-point static bending was carried out on tensile-testing machine ZD-40. Loading was performed normal to a track plane as well as along the line tangent to it according to the schemes on Figure 2. First loading of P1 = 300 kN force was carried out normal to the track plane (Figure 2, a). If after such loading there were not found the signs of loss of metal integrity (crack appearance), regardless the presence of the residual stresses, then the track was loaded with P2 = –300 kN force (in direction opposite to a force application relatively to first loading (Figure 2, b). The next shear

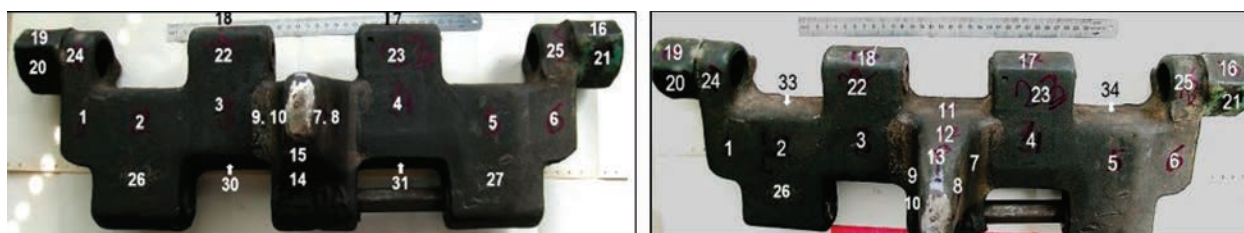
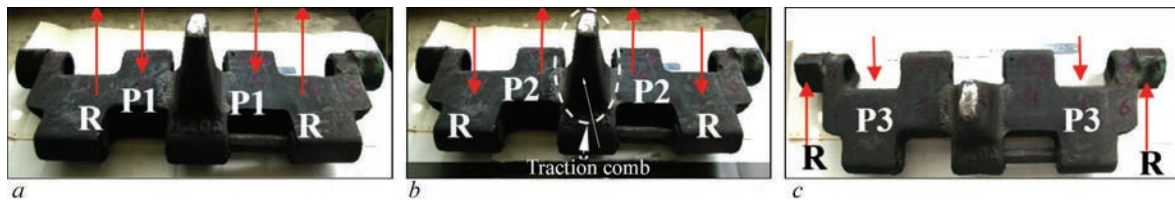


Figure 1. General view of tracks before testing



**Figure 2.** Schemes of loading of track at 4-point static bend tests [5]

loading at 4-point force application after previous loadings was carried out along the tangent line to the track plane of  $P3 = 240$  kN force (Figure 2, c).

Under operation conditions the track is affected by roller forces ( $P$ ) which being equalized by ground pressure ( $R$ ). In this case the scheme of track loading corresponds to 4-point bend. Operation provokes deformation and hardening of the metal surface layers, including due to contact stresses, taking into account a traction guide lug, which takes forces of a drive gear and the side forces from the suspension rollers during manoeuvres of a vehicle. Nonuniform stress-strain state of different track sections occurs under operation conditions and at bend tests. The most deformed are the metal surface layers. However, due to high ductility of metal in initial condition of the steel as a result of ductility deformation during operation there is a redistribution of stresses in the most stressed areas with neighbor areas that provides structure integrity.

A reference caterpillar track and the experimental tracks, made of metal with some deviations of composition from standard one (tracks Nos 1–4 (2021), Nos 7–8 (2020) 1–5 (2021) and ZP-1, ZP-2 (2021) were subjected to 4-point bend tests. Year of test is given in brackets.

Analysis of composition of the tracks metal was carried out on photoelectric spectrometer Spectrovac-1000 (Baird). Composition of metal of the investigated tracks and steel 110G13L is given in Table 3.

As can be seen from Table 3 the examined experimental tracks from different manufacturers vary by percent of certain chemical elements (C, Si, Mn, Cr, P) between themselves as well as from ones regulated by the normative documents for steel 110G13L.

## RESULTS OF EXPERIMENTAL INVESTIGATIONS AND THEIR ANALYSIS

Present work provides the results of comparison of structural state of metal of the experimental caterpillar tracks of different manufacturers with the reference one by the results of coercive force measurement. Figure 3 shows the typical distribution diagrams of coercive force measured with structurescope in the different points of surface of the reference track in initial condition and after testing in different planes. It should be noted that in the main part of the track (for example, points 1–6, Figure 3, a) after three loadings by schemes 1–3 (Figure 2) there were no dramatic changes of the structural state where the value of coercive force was equal zero. The most loaded is the metal of traction comb (points 8, 9, Figure 3, b) and points 33 and 34 (Figure 3, c) in the main part of the track.

Microstructure of fragments of the examined reference track in initial condition in different zones is characterized with austenite of mixed grain-dendrite morphology (cast structure) (Figure 4, a) and austenite of grain morphology (Figure 4, b) without the signs of microplastic deformation.

The reference track with optimum structural state of metal (austenitic structure, Figure 4) in initial condition is characterized with absence of magnetic properties that is proved by the coercive force measurements ( $H_c = 0$  A/cm). In contrast to the reference track the different areas of the experimental tracks 1–4 (2021) in initial condition had sufficiently high values of coercive force that is related with appearance of ferromagnetic phases.

Concerning the microstructure of other examined samples, despite different grains, etching revealed

**Table 3.** Composition of metal of examined caterpillar tracks and steel 110G13L

Track number	Weight fraction, %										
	C	Si	Mn	Cr	Ni	Cu	Mo	Ti	V	S	P
Standard	1.09	0.91	13.3	0.90	0.96	0.21	0.19	0.015	0.068	0.014	0.035
1–4 (2021)	1.04	1.25	2.30	1.52	0.33	0.16	<0.1	<0.05	0.036	0.02	0.15
1–5 (2021)	0.44	0.75	15.8	0.71	0.72	0.11	0.056	0.017	0.006	0.015	0.019
7–8 (2020)	0.66	0.34	12.6	0.63	0.18	0.11	0.038	<0.01	0.017	0.016	0.070
ZP-1, ZP-2	0.35	0.42	16.8	1.10	0.080	0.045	0.055	<0.01	0.022	0.013	0.028
Steel 110G13L (DSTU 8781:2018)	0.9–1.5	0.3–1.0	11.5–14.5	1.0 not more than	1.0 not more than	–	–	–	–	0.05	0.12
GOST 2176–77	0.9–1.4	0.8–1.0	11.5–15.0	Up to 1	Up to 1	Up to 0.3	–	–	–	Up to 0.05	Up to 0.12

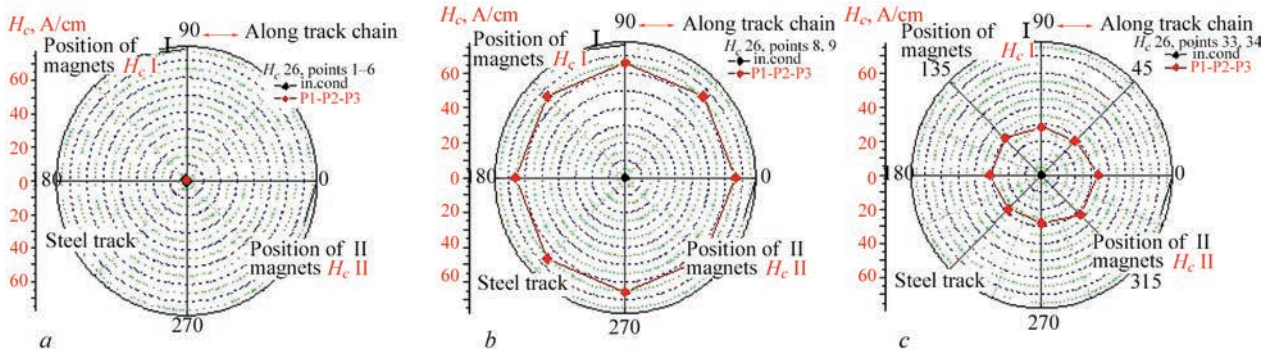


**Figure 3.** Typical distribution diagrams of the coercive force in different points of surface of the reference track in initial condition and after tests: *a* — points 1–6; *b* — points 8, 9; *c* — points 33, 34.  $H_c$  values in initial condition are shown by black and after loading by red. Number of points corresponds to Figure 1

the surface layers (of 300–400  $\mu\text{m}$  thickness) with the signs of microplastic deformation (Figure 5, *a*) in addition to austenite grain morphology. Martensite ( $\alpha$ -phase) in different amount respectively for each of the examined samples was detected in the austenite grains of hardened layers between the slip bands. It explains appearance of ferromagnetic properties in these samples of austenite steel. It was found that the values of coercive force rises with increase of portion of  $\alpha$ -phase, percent of which was determined using ferritometer of local type Ferrit Gehalt-messer-1.053.

Absence of increase of the coercive force at regulated loads by scheme 1 (Figure 2, *a*) corresponding to the initial condition indicates invariability of structural

state of metal at deformation (Figure 6). It is necessary to note the significant scatter of the absolute values of coercive force in the subsurface layers of the different tracks that is a reflection of metal structural state. Thus, within the range of batch of tracks 1–4 (2021): for metal of track No. 1 the absolute values of coercive force of different areas lied in the limits of 21.1–70.5 A/cm; track No. 2 — 29.7–77.6 A/cm; track No. 3 — 4.6–68.1 A/cm; track No. 4 — 14.2–62.7 A/cm.

4-point bend tests showed that tracks 1–4 (2021) withstood only 50 % of the reference load, in other words metal had very low resistance to such loading. At that failure had brittle nature without the signs of

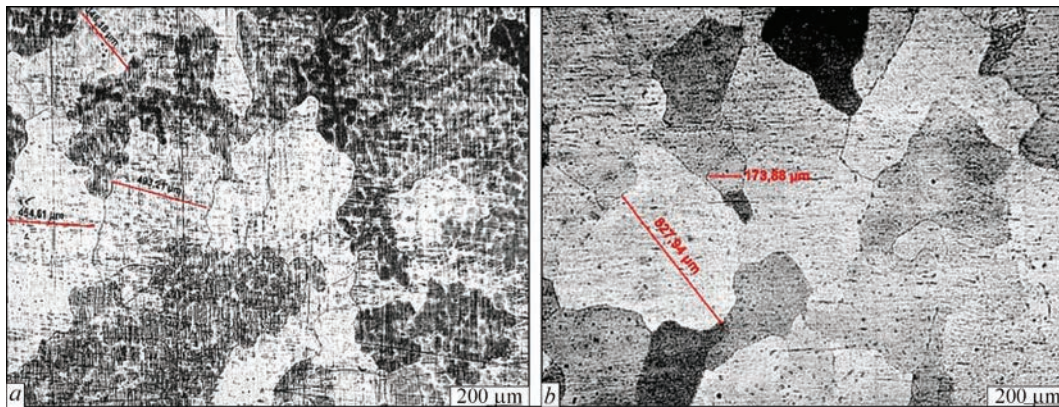


**Figure 4.** Example of microstructure of fragments of the examined reference track in initial condition in different zones ( $\alpha$ -phase  $\sim 0\%$ ,  $H_c = 0$  A/cm)

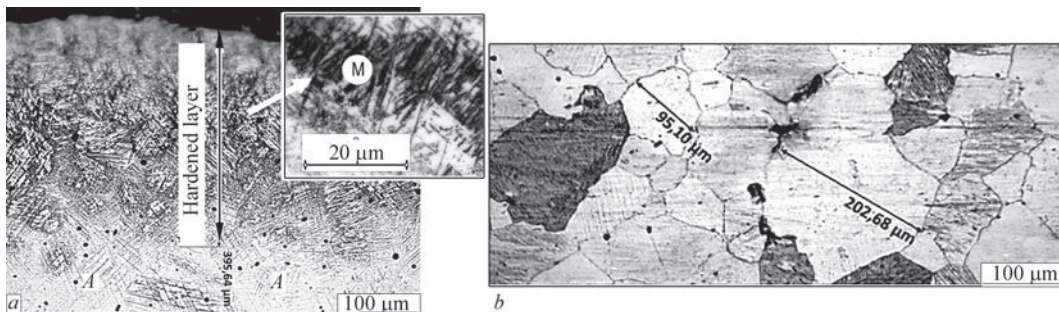


**Figure 5.** Examples of typical microstructure of the examined experimental tracks (in the cross-section) in initial condition in different zones: *a* — near-boundary (hardened) layer,  $\alpha$ -phase  $\sim 0.3$ – $0.6\%$ ,  $H_c = 35$  A/cm; *b* — austenite base,  $\alpha$ -phase  $\sim 0\%$ ,  $H_c = 0$  A/cm; M — martensite ( $\alpha$ -phase)

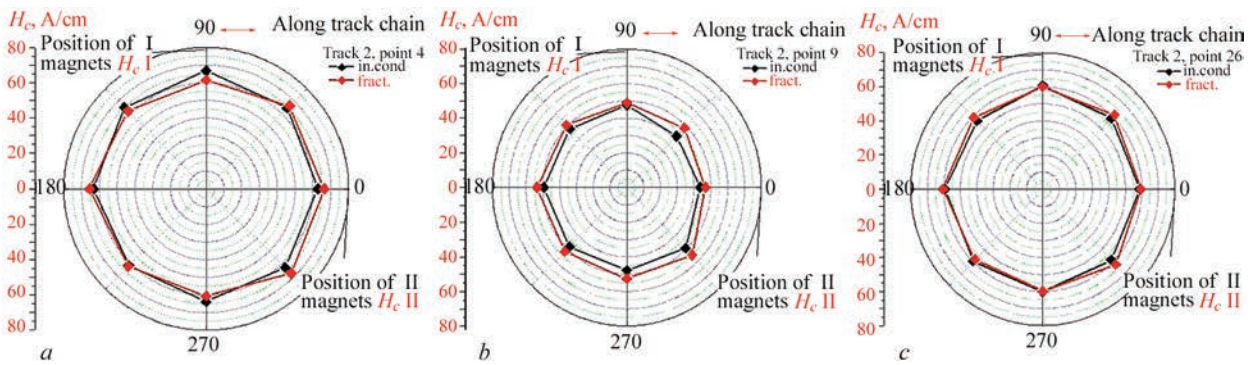


**Figure 6.** Typical distribution diagrams of the coercive force in different points of surface of the experimental tracks 1–4 (2021) in initial condition and after tests by scheme 1 (Figure 2, a): a — point 4; b — point 9; c — point 26



**Figure 7.** General view of integrity loss (crack formation) of metal of tracks 1–4 (2021) after 4-point bend tests

plastic deformation (including the presence of residual deflection (Figure 7)).

In contrast to the examined tracks 1–4 (2021) the structural state of the experimental tracks 1–5 (2021) (Figure 8) differs by presence of the zones with zero values of coercive force that is typical for austenite structure. Examined tracks 1–5 (2021) as well as tracks 1–4 (2021) are characterized with absence of increase of the values of coercive force at rated loads relatively to the initial condition that indicates invariability of the metal structural state at deformation. A brittle nature of fracture proves absence of metal ductility margin. At that the tracks at loading by schemes 1 and 3 (Figure 2, a, c) withstood rated loading. At loading by scheme 2 (Figure 2, b) the track withstood only 17.7 t of 30 t being rated.

Insignificant increase of the values of coercive force at loading and appearance of plastic deformation signs (slip bands) were found on the surface of tracks 7–8 (2020) in contrast to the mentioned above tracks 1–5 (2021) and 1–4 (2021). At that the tracks withstood the rated loadings with certain values of residual deflection in corresponding planes of the loading. Figure 9 demonstrates the typical distribution diagrams of coercive force in the different points of the surface of experimental tracks 7–8 (2020) in initial condition and after 4-point bend tests.

It also necessary to note a scatter of the absolute values of coercive force, which in initial condition for the experimental tracks 7–8 (2020) lied in 14.3–67.1 A/cm range. However, increase of the values of coercive force took place after tests in the most loaded points of the tracks that allowed evaluating the level of metal damage in deformation [5].

Examined tracks of the other manufacturer (tracks ZP-1 and ZP-2) are also characterized with presence of sufficiently high values of the coercive force and their non-uniform distribution in the different points in initial condition (Figure 10). For comparison Figure 10 shows also the distribution diagrams of coercive force after the rated loadings.

Structural state of metal of tracks ZP-1 and ZP-2 in initial condition, evaluated by the value of coercive force, corresponds approximately to tracks 1–5

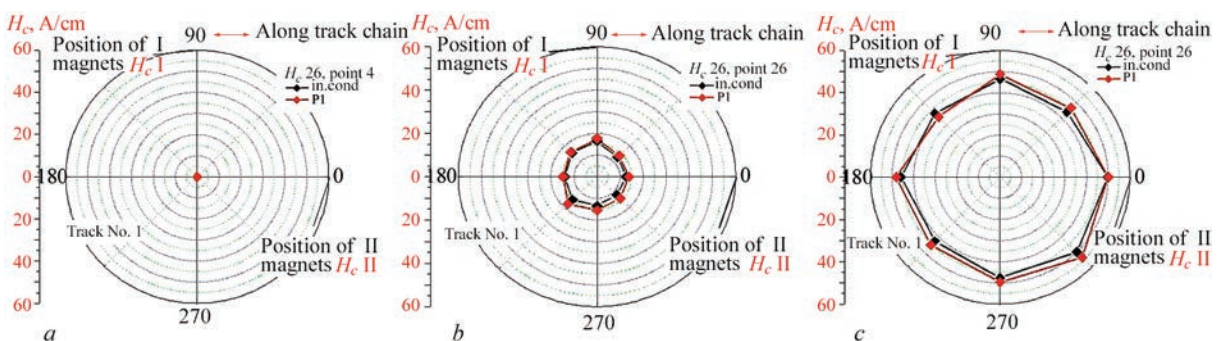


**Figure 8.** Typical distribution diagrams of the coercive force in different points of surface of experimental tracks 1–5 (2021) in initial condition and after tests: a — track No. 1 point 4; b — tracks No. 2 point 6; c — track No. 1 point 26.  $H_c$  values in initial condition are shown by black and after loading by red

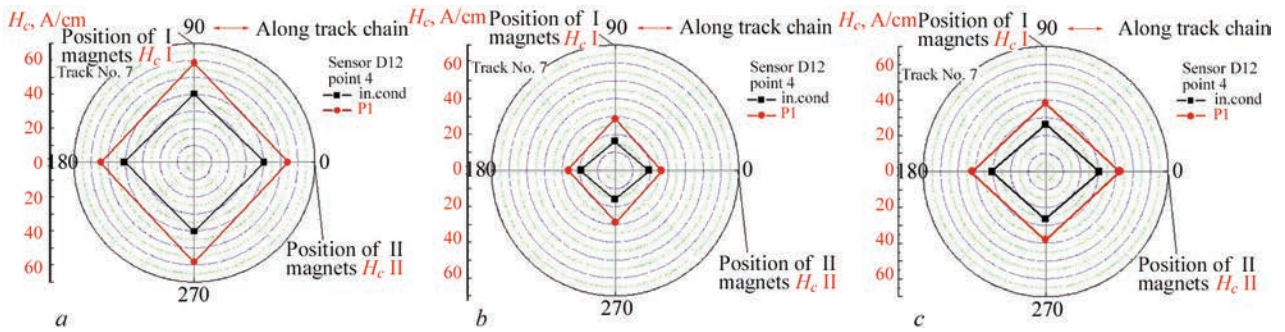


**Figure 9.** Typical distribution diagrams of the coercive force in different points of surface of experimental track 7–8 (2020) in initial condition and after tests: *a* — point 4; *b* — point 9; *c* — point 26.  $H_c$  values in initial condition are shown by black and after loading by red

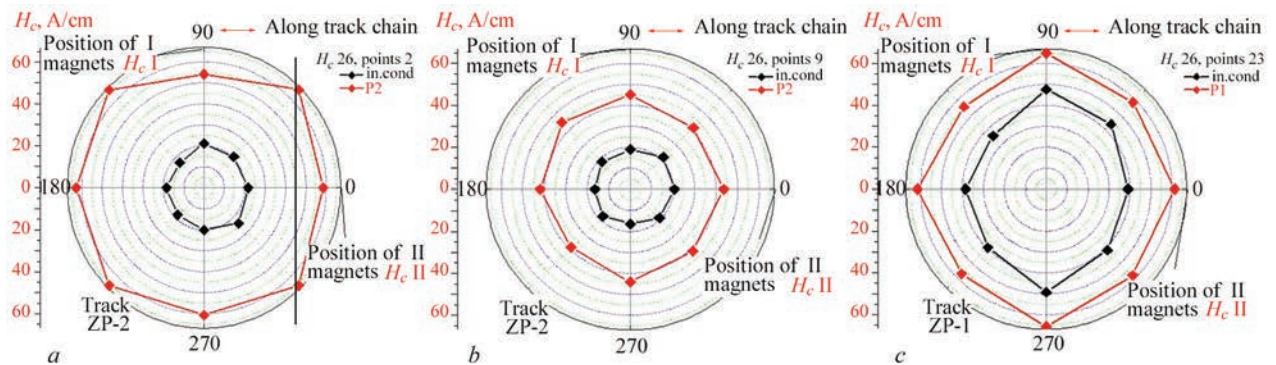


**Figure 10.** Typical distribution diagrams of the coercive force in different points of surface of experimental tracks ZP-1 and ZP-2 in initial condition and after tests: *a* — track ZP-2 point 2; *b* — track ZP-2 point 9; *c* — track ZP-1 point 23.  $H_c$  values in initial condition are shown by black and after loading by red

(2021), 1–4 (2021) and 7–8 (2020). However, for metal of tracks ZP-1 and ZP-2 significant increase of the values of coercive force is typical under the rated loadings relatively initial condition. Significant deformation of tracks took place at 4-point bend loading. Metal had sufficient ductility margin for deformation that resulted in redistribution of loads in the most loaded zone and increased fracture resistance. On loading of tracks ZP-1 and ZP-2 by schemes 1 and 2 (Figure 2, *a, b*) plastic deformation started in 24.6 t loading and fracture at 28.9 t.

The authors [1] based on the systematic researches proposed the optimum indices of relationship of elements for steel 110G13L, namely  $Mn/C \leq 10$  and  $P + 0.4C \geq 0.5\%$ , where growth of Mn/C index provokes increase of impact toughness and the optimum values of Mn/C are in 12–13 range. Rise of  $P + 0.4C$  index above 0.5% provokes increase of steel susceptibility to crack formation.

Indices Mn/C and  $P + 0.4C$  of metal of investigated by us tracks in comparison with the optimum ones [1] are represented in Table 4.

Thus, the metal of all examined experimental tracks does not correspond to the requirements as for composition of steel 110G13L according to reference documents (Table 3) and as for the optimum ranges of indices Mn/C and  $P + 0.4C$  (Table 4), that found rep-

resentation on the distribution diagrams of coercive force of the experimental tracks in initial condition.

In addition to the outlined above possibilities of application of the coercimetric testing the developed approach can be used for evaluation of quality of the products of austenite steels for determination of damages obtained in the process of testing or operation [6, 7]. According to it in monitoring of the structural state it is necessary to pay attention not on the maximum values of coercive force, but on process kinetics. Due to static or cyclic operating time the dependence of coercive force on accumulated damages has ascending and descending areas. An area of increase of the coercive force values corresponds to crack nucleation stage and area of their values decrease matches with the stage of crack propagation due to metal integrity loss at pores and crack formation.

Use of coercimetric testing allows performing evaluation of the metal quality in initial condition as well as the level of loading and obtained damages at any of stages in any point of products under operation

**Table 4.** Indices Mn/C and  $P + 0.4C$  of metal of examined tracks in comparison with optimum ones [1]

Index	[1]	Reference	1–4 (2021)	7–8 (2020)	1–5 (2021)	ZP-1, ZP-2
Mn/C	12–13	12.2	2.21	19.1	35.9	48.0
$P+0.4C, \%$	$\leq 0.5$	0.471	0.566	0.334	0.195	0.164

condition by means of measurement of the coercive force values.

## CONCLUSIONS

There were carried out a nondestructive testing diagnostics of a structural state (by coercive force measurements) of metal of 13 experimental caterpillar tracks of different manufacturers in initial condition and after standard 4-point bend tests.

The structural state of metal of ZP-1 and ZP-2 tracks in initial condition, evaluated by the value of coercive force approximately corresponds to tracks 1–5 (2021), 1–4 (2021) and 7–8 (2020). However, metal of tracks ZP-1 and ZP-2 is characterized with significant increase of the values of coercive force at rated loads relatively initial condition. Significant deformation of the tracks took place at 4-point bend loading. The metal had sufficient ductility margin for deformation that promoted redistribution of loads in the most loaded zone and increased fracture resistance.

In contrast to the reference track the various areas of the experimental tracks 1–4 (2021) and 1–5 (2021) in initial condition had sufficiently high values of coercive force that is related with unconformity of composition and heat treatment to the reference requirements. The metal of mentioned tracks had understated ductility that did not contribute to redistribution of the maximum stresses in the most loaded areas and resulted in brittle fracture after standard 4-point bend tests.

It also necessary to note scatter of the absolute values of coercive force, which in initial condition for experimental tracks 7–8 (2020) lied in 14.3–67.1 A/cm range. However, the most loaded points of the tracks after tests demonstrated increase of the coercive force values that allows evaluating the level of metal damage in deformation [5].

Obtained experimental results of 4-point bend tests of the experimental tracks of austenite steel of Hadfield type with certain deviations of composition from the regulated one proved the possibility of application of nondestructive coercimetric testing for evaluation of initial structural state and level of loading of metal which characterizes the level of obtained damages after loading by the results of coercive force measurement.

## REFERENCES

1. Davydov, N.G. (1979) *High-manganese steel*. Moscow, Metallurgiya [in Russian].
2. Solntsev, Yu.P., Andreev, A.K., Grechin, R.I. (1991) *Cast cold-resistant steels*. Moscow, Metallurgiya [in Russian].
3. Zimokos, G.N., Adamenko, L.A., Ivanova, L.Kh. (2011) Influence of chemical composition on the properties of high-manganese steel in armored steel castings of cone crushers. *Metallurgicheskaya i Gornorudnaya Promyshlennost*, **4**, 140 [in Russian].
4. Sharov, N.V., Platonov, A.V., Chumakov, V.A. (2012) Production and quality assessment of castings of rapidly-wearing parts from high-manganese steels. *Gornaya Promyshlennost*, **3**, 18–28 [in Russian].
5. Gopkalo, O.P., Zemtsov, M.P., Gopkalo, O.Ye. et al. (2021) Diagnosis of damage to caterpillar tracks under mechanical loading based on the results of measurement of the coercive force. *Tekh. Diahnost. ta Neruiv. Kontrol*, **1**, 17–26 [in Ukrainian]. DOI: <https://doi.org/10.37434/tdnk2021.01.03>
6. Gopkalo, O.P., Nekhotiashchii, V.O., Bezlyudko, G.Ya. et al. (2019) Diagnosis of damage in austenitic steel AISI 304 at mechanical loading by measurements of coercive force. *Tekh. Diahnost. ta Neruiv. Kontrol*, **4**, 12–24 [in Ukrainian]. DOI: <https://doi.org/10.37434/tdnk2019.04.01>
7. Gopkalo, O., Bezlyudko, G., Nekhotiashchii, V. et al. (2020) Damage evaluation for AISI 304 steel under cyclic loading based on coercive force measurements. *Int. J. Fatigue*, **139**. DOI: <https://doi.org/10.1016/j.ijfatigue.2020.105752>

## ORCID

O.P. Gopkalo: 0000-0001-7799-3870

## CONFLICT OF INTEREST

The Authors declare no conflict of interest

## CORRESPONDING AUTHOR

O.P. Gopkalo

E.O. Paton Electric Welding Institute of the NASU  
11 Kazymyr Malevych Str., 03150, Kyiv, Ukraine.

E-mail: [apg1947@ukr.net](mailto:apg1947@ukr.net)

## SUGGESTED CITATION

O.P. Gopkalo, O.Ye. Gopkalo, M.P. Zemtsov, Ye.V. Kovalenko, V.E. Bodunov (2022) Express-evaluation of the quality of producing caterpillar tracks by the results of coercive force measurement. *The Paton Welding J.*, **11**, 45–52.

## JOURNAL HOME PAGE

<https://patonpublishinghouse.com/eng/journals/tpwj>

Received: 06.10.2022

Accepted: 29.12.2022